

Original Research

Inhibition of BCL2A1 by STAT5 inactivation overcomes resistance to targeted therapies of *FLT3*-ITD/D835 mutant AML

Kotoko Yamatani^a, Tomohiko Ai^a, Kaori Saito^a, Koya Suzuki^a, Atsushi Hori^{a,b}, Sonoko Kinjo^c, Kazuho Ikeo^c, Vivian Ruvolo^d, Weiguang Zhang^d, Po Yee Mak^d, Bogumil Kaczkowski^e, Hironori Harada^f, Kazuhiro Katayama^g, Yoshikazu Sugimoto^h, Jered Myslinskiⁱ, Takashi Hatoⁱ, Takashi Miida^a, Marina Konopleva^j, Yoshihide Hayashizaki^k, Bing Z. Carter^d, Yoko Tabe^{a,d,l,1,*}, Michael Andreeff^{d,*}

^a Department of Clinical Laboratory Medicine, Juntendo University Graduate School of Medicine, 2-1-1 Hongo, Bunkyo-ku, Tokyo 113-8421, Japan

^b Center for Genomic and Regenerative Medicine, Juntendo University Graduate School of Medicine, Tokyo, Japan

^c Center for Information Biology, National Institute of Genetics, Shizuoka, Japan

^d Department of Leukemia, Section of Molecular Hematology and Therapy, The University of Texas MD Anderson Cancer Center, 1515 Holcombe Boulevard, Unit 448, Houston, TX 77030, United States

^e Preventive Medicine and Diagnosis Innovation Program, RIKEN Center for Life Science Technologies, Kanagawa, Japan

^f Department of Hematology, Juntendo University Graduate School of Medicine, Tokyo, Japan

^g Laboratory of Molecular Targeted Therapeutics, School of Pharmacy, Nihon University, Chiba, Japan

^h Division of Chemotherapy, Faculty of Pharmacy, Keio University, Tokyo, Japan

ⁱ Department of Medicine, Indiana University School of Medicine, Marion, IN, United States

^j Department of Leukemia, Section of Leukemia Biology Research, The University of Texas MD Anderson Cancer Center, Houston, TX, United States

^k Kabushiki Kaisya Dnaform, Yokohama, Japan

^l Department of Next Generation Hematology Laboratory Medicine, Juntendo University Graduate School of Medicine, Tokyo, Japan

ARTICLE INFO

Keywords:

BCL2A1
AML
FLT3
CAGE
Venetoclax

ABSTRACT

Tyrosine kinase inhibitors (TKIs) are established drugs in the therapy of *FLT3*-ITD mutated acute myeloid leukemia (AML). However, acquired mutations, such as D835 in the tyrosine kinase domain (*FLT3*-ITD/D835), can induce resistance to TKIs. A cap analysis gene expression (CAGE) technology revealed that the gene expression of *BCL2A1* transcription start sites was increased in primary AML cells bearing *FLT3*-ITD/D835 compared to *FLT3*-ITD. Overexpression of *BCL2A1* attenuated the sensitivity to quizartinib, a type II TKI, and venetoclax, a selective BCL2 inhibitor, in AML cell lines. However, a type I TKI, gilteritinib, inhibited the expression of *BCL2A1* through inactivation of STAT5 and alleviated TKI resistance of *FLT3*-ITD/D835. The combination of gilteritinib and venetoclax showed synergistic effects in the *FLT3*-ITD/D835 positive AML cells. The promoter region of *BCL2A1* contains a BRD4 binding site. Thus, the blockade of BRD4 with a BET inhibitor (CPI-0610) downregulated *BCL2A1* in *FLT3*-mutated AML cells and extended profound suppression of *FLT3*-ITD/D835 mutant cells. Therefore, we propose that *BCL2A1* has the potential to be a novel therapeutic target in treating *FLT3*-ITD/D835 mutated AML.

Introduction

Acute myeloid leukemia (AML) is associated with chromosomal disorders, germline, and somatic driver mutations [1]. Specifically, internal tandem duplications in the juxtamembrane domain of the

FMS-like tyrosine kinase 3 gene (*FLT3*-ITD) and missense mutations in the tyrosine kinase domain (TKD) of the *FLT3* gene play critical roles in the pathophysiology of AML. In fact, *FLT3*-ITD and *FLT3*-TKD mutations were detected in approximately 15–35% and 5–10% of AML patients, respectively [2], and approximately 1–3% of the patients carry both

* Corresponding authors at: Department of Leukemia, Section of Molecular Hematology and Therapy, The University of Texas MD Anderson Cancer Center, 1515 Holcombe Boulevard, Unit 448, Houston, TX 77030, United States.

E-mail addresses: tabe@juntendo.ac.jp (Y. Tabe), mandreeff@mdanderson.org (M. Andreeff).

¹ These authors contributed equally to this work.

mutations at diagnosis [3,4]. Both *FLT3*-ITD and *FLT3*-TKD mutations constitutively activate *FLT3* tyrosine kinase, leading to uncontrolled activation of downstream signaling pathways including phosphoinositide 3-kinase (PI3K), mitogen-activated protein kinases (RAS-MAPK), and STAT5 [5].

Several *FLT3*-directed tyrosine kinase inhibitors (TKIs) have been developed for treatment of *FLT3*-mutated AML. These inhibitors can be divided into two distinct functional subtypes based on their mechanism of action. Type I inhibitors, such as gilteritinib, midostaurin, and crenolanib block the active and inactive conformation of *FLT3* targeting the ITD and TKDs, while the type II inhibitors, such as quizartinib and sorafenib, selectively bind to the inactive state of *FLT3*-ITD only [5,6]. TKIs have shown favorable effects in refractory *FLT3*-mutated AML compared to traditional chemotherapies [7,8], and the combination of TKIs with Ara-c and idarubicin or daunorubicin also showed promising outcomes in newly diagnosed *FLT3* mutant AML [9]. Thus, the FDA approved midostaurin and gilteritinib for clinical use [10,11]. However, the effects of TKIs are often transient, resulting in disease relapse after initial responses [12].

Multiple underlying resistance mechanisms against these TKIs have been proposed. One mechanism is that the TKI-induced acquisition of additional point mutations in the TKD accounts for resistance of *FLT3*-ITD cells. Another is the co-existence of multiple mutated clones including *FLT3*-ITD and *FLT3*-TKD prior to treatment, which causes proliferation of refractory clones after TKI treatments. Targeted sequencing of single cells derived from patients with relapsed/refractory AML showed polyclonal blast populations harboring several subclones with ITD plus D835 mutations in the activation loop of TKD, such as D835V, D835Y, or D835F (*FLT3*-ITD/D835) [13], which might contribute to subsequent leukemia progression.

On the other hand, *FLT3*-independent alternative signaling pathways can lead to resistance. Type I TKIs were found to be more effective in AML with *FLT3*-ITD/TKD mutations compared to type II TKIs. However, type I TKI-induced mutations in the *RAS* gene have been identified as an important factor of *FLT3*-independent resistance [14]. Also, *FLT3*-ITD/TKD double mutant clones have been reported to activate alternative survival pathways involved in DNA repair and anti-apoptosis during leukemia progression [15,16].

To overcome resistance, combination therapies with inhibitors against *FLT3* and alternative resistance factors such as apoptosis have been developed [17]. A phase Ib/II clinical trial using quizartinib with a specific *BCL2* inhibitor, venetoclax (NCT03735875), and a phase Ib multi-center clinical study of gilteritinib and venetoclax (NCT03625505) have been reported in relapsed/refractory AML patients with *FLT3* mutations. Initial results of these studies revealed promising outcomes [18,19].

Characteristics of signaling pathways in the *FLT3*-ITD/TKD double mutations remain poorly understood. This study aims to investigate the survival mechanisms of AML cells with *FLT3*-ITD/TKD mutations. AML samples from patients bearing *FLT3*-ITD/TKD mutations were analyzed by transcriptome analysis and compared with those with *FLT3*-ITD only. Cap analysis gene expression (CAGE) technology revealed that *FLT3*-ITD/TKD AML showed higher levels of anti-apoptotic *BCL2A1* gene transcripts, which is associated with resistance to venetoclax [20,21], compared to *FLT3*-ITD AML cells and thus, overexpression of *BCL2A1* in *FLT3*-ITD AML cells decreases the sensitivity to quizartinib. Based on these findings, we propose *BCL2A1* as a novel therapeutic target in refractory AML with *FLT3*-ITD/D835.

Materials and methods

Preparation of cell lines and primary AML cells

Human MV4;11 cells (RRID: CVCL_0064) were purchased from the American Type Culture Collection (Manassas, VA), and Molm13 cells (RRID: CVCL_2119) were purchased from DSMZ (Braunschweig,

Germany). These cells were cultured in IMDM or RPMI 1640 medium supplemented with 10% heat-inactivated FBS, 100 U/mL penicillin, and 100 µg/mL streptomycin. MV4;11 cells bearing *FLT3*-ITD/D835 mutations (MV4;11-ITD/D835) were established from parental MV4;11 bearing *FLT3*-ITD mutation (MV4;11-ITD) by exposure to quizartinib at incremental concentrations of from 0.3 to 1.5 nM for six months, followed by clone cultures [22]. The *FLT3*-ITD/D835 mutations were confirmed by direct sequencing. The established *FLT3*-ITD/D835 clone had a 50% inhibitory concentration (IC₅₀) of 6.7 nM for quizartinib, which was 34-times higher than that of MV4;11-ITD. MV4;11 cells bearing *FLT3*-ITD/D835 mutations were maintained in IMDM containing quizartinib (1.5 nM). Quizartinib was removed three to four days before experiments.

To stably overexpress *BCL2A1* in AML cell lines, a lentiviral vector was used for gene delivery. A lentiviral transfection vector with the *BCL2A1* open reading frame (RefSeq NM_004049.4) under regulation of the human EF1A promoter was purchased from Vector Builder (Chicago, IL). As a negative control, a lentiviral transfection vector was used with a 300 bp non-coding stuffer sequence under the same promoter from the same vendor. Lentivirus was prepared by transient co-transfection of HEK-293T cells (ATCC, RRID: CVCL_0063) with an equimolar mix of transfer vector and packaging plasmids (psPAX2 and pMD2.G, RRID: Addgene_12,260 and RRID: Addgene_12,259, respectively, from Addgene) using JetPrime transfection reagent as directed by the manufacturer (Polyplus, Illkirch, France). Lentiviral supernatants were harvested 48-h post transfection and passed through 0.45-micron, surfactant-free-cellulose acetate membranes. AML cell lines were incubated with undiluted viral supernatant overnight at 37 °C under 5% CO₂; infected cells were then washed and selected with puromycin (Invivogen, San Diego, CA) at 0.5 µg/mL. Increased expression of each transgene was verified by immunoblot analysis.

Primary peripheral blood and bone marrow (BM) samples were obtained from newly diagnosed or relapsed AML patients ($n = 26$) after written informed consent was obtained in accordance with the University of Texas MD Anderson Cancer Center Institutional Review Board regulations under the Declaration of Helsinki principles. The protocol was approved by the respective Institutional Ethics Committees. The patients carrying nucleophosmin (NPM1) mutations were excluded since *NPM1* mutations are associated with favorable prognosis in negative or low allelic ratio *FLT3*-ITD AML. Their age varied from 24 to 87 years. Ficoll-Hypaque density gradient centrifugation was used to separate mononuclear cells (Sigma-Aldrich, St Louis, MO). Venetoclax (ABT-199/GDC-0199) and quizartinib (AC220) were purchased from Selleck-chem (Houston, TX). Gilteritinib and CPI-0610 were purchased from Funakoshi (Tokyo, Japan) and Abcam (Cambridge, UK), respectively.

Analyses of cell viability and apoptosis

Cell proliferation was assessed by Cell Counting Kit-8 (WST-8, Dojindo, Kumamoto, Japan). Effects of the reagents on cellular proliferation were evaluated as percent-decrease of cell viability compared to the cell viability in the culture medium containing 0.01% dimethyl sulfoxide. The half-maximal inhibitory concentration (IC₅₀) and combination index (CI) were calculated by the Chou-Talalay method based on the median-effect principle [23], using CalcuSyn 2.0 software (Bio-software, Cambridge, UK). The dosage of each reagent was determined based on the previously reported therapeutic concentrations in humans: 270 nM for quizartinib [24], 310 nM for gilteritinib [25], 2.5 µM for venetoclax [26], and 6 µM for CPI-0610 [27].

Immunoblot analysis

Immunoblot analysis was performed as previously described [28]. For immunoblotting, the following antibodies were used: b-actin (Sigma-Aldrich, St. Louis, MO, Cat# A5316, RRID:AB_476,743); MCL-1 (BD

Biosciences, San Diego CA, Cat# 559,027, RRID:AB_397,176); BCL2 (Cell Signaling Technology, Danvers, MA Cat# 2872, RRID:AB_10,693,462), BCL2A1 (Cell Signaling Technology, Cat# 14,093, RRID:AB_2,798,390), BCL-XL (Cell Signaling Technology, Cat# 2762, RRID:AB_10,694,844), STAT5 (Cell Signaling Technology, Cat# 9363, RRID:AB_2,196,923), phosphorylated (p-) STAT5 (Cell Signaling Technology, Cat# 9351, RRID:AB_2,315,225), horseradish peroxidase-linked anti-mouse (Cell Signaling Technology, Cat# 7076, RRID:AB_330,924) and anti-rabbit IgG (Cell Signaling Technology, Cat# 7074, RRID:AB_2,099,233).

Mutational analyses

Mutation screening was performed using paired-end sequencing on the MiSeq sequencer (Illumina, San Diego CA) using DNA from fresh BM samples or peripheral blood. NGS sequencing libraries were created by polymerase chain reaction (PCR) amplification of target regions using TruSeq chemistry (Illumina) or Haloplex probe capture followed by PCR amplification of target regions using Haloplex chemistry (Agilent, Santa Clara, CA). The panel interrogated either selected hotspot or entire coding regions of 25 genes (*ASXL1*, *BRAF*, *CEBPA*, *DNMT3*, *EGFR*, *EZH2*, *GATA1*, *GATA2*, *IDH1*, *IDH2*, *IKZF2*, *JAK2*, *KIT*, *MDM2*, *MLL*, *MPL*, *MYD88*, *NOTCH1*, *PDGFRA*, *PTPN11*, *RAS*, *RUNX1*, *TET2*, *TP53*, *WT1*) utilizing TruSeq Amplicon Cancer Panel kit (Illumina) as described previously [29]. Human genome build 19 (hg19) was used as the reference for sequence alignment. Reporter and Agilent SureCall were used for variant calling for TruSeq and Haloplex workflows, respectively. *FLT3*-ITD and *FLT3*-TKD mutation testing was performed using PCR followed by capillary electrophoresis on Genetic Analyzer (Applied Biosystems, Foster City, CA), as described previously [30].

mRNA quantification

Total RNA was extracted from cells with the RNeasy Mini Kit (Qiagen, Hilden, Germany). First-strand cDNA was synthesized with oligo (dT) as primer (Superscript II System; Invitrogen). Real-time reverse-transcriptase PCR (RT-PCR) was performed by the Model 7500 Real-time PCR System (Applied Biosystems). Expression of the mRNAs encoding *BCL2*, *BCL2A1*, and *GAPDH* was detected by TaqMan Gene Expression Assays (*BCL2*: Hs00608023_m1; *BCL2A1*: Hs00187845_m1; *GAPDH*: Hs99999905_m1; Applied Biosystems). The expression of each gene transcript relative to that of *GAPDH* was calculated as follows: relative expression = $100 \times 2^{\exp[-\Delta C_t]}$, where ΔC_t is the mean C_t of the transcript of interest minus the mean C_t of the transcript for *GAPDH*. The C_t data from duplicate PCRs were averaged for calculation of relative expression.

CAGE

CAGE libraries from the RNA samples were prepared as described previously [31]. CAGE peaks that represent transcription start sites were defined by the decomposition-based peak identification method and annotated to genes [32]. Peaks were given a name in the form pN@GENE, where GENE indicates gene name and N indicates the rank in the ranked list of promoter activities for that gene. For example, p1@BCL2 represent the highest expression among alternative promoters among the peaks associated with *BCL2* gene, according to the FANTOM5 CAGE profiles [32]. The relative log expression method was utilized to calculate normalization factors for the expression of promoters. Normalized data were subjected to the R Bioconductor package “edgeR” for differential expression (Bioconductor, RRID:SCR_006442). Then, gene ontology (GO) analysis of differentially expressed genes was performed with DAVID Bioinformatics Resources (DAVID, RRID:SCR_001881) [33].

RNA-Seq analysis

Sequencing libraries were generated using NEBNext Ultra RNA Library Prep Kit for Illumina (New England Biolabs, Ipswich, MA) following the manufacturer’s recommendations. The library fragments were purified with QIAquick PCR kits (QIAGEN). The clustering of the index-coded samples was performed on a cBot cluster generation system using HiSeq PE Cluster Kit v4-cBot-HS (Illumina) according to the manufacturer’s instructions. After cluster generation, the libraries were sequenced on an Illumina platform and 150 bp paired-end reads were generated.

The reads were aligned to the GRCh38/hg38 genome reference and indexed using STAR aligner (STAR, RRID:SCR_004463) and Samtools (SAMTOOLS, RRID:SCR_002105) with default parameters. VarDict, an RNA-sequencing data compatible variant caller, was used with default settings to identify edited regions. Edits were searched for against hg38 genome FASTA (FASTA, RRID:SCR_011819) and RefSeq (RefSeq, RRID:SCR_003496) hg38 bed file references with a minimum allele frequency of 0.01. Only single nucleotide mutations were kept. The output was further filtered by keeping edits occurring in exons (biomaRt) with > 100 reads in each experiment, > 0.1 differences in allele frequency of high-quality bases between the experimental conditions (higher in MV4;11 with *FLT3*-ITD/D835 vs. *FLT3*-ITD). Sites corresponding to A-to-I edit sites were removed from the list using REDIttools (REDIttools, RRID:SCR_012133) [34]. Finally, the list of edit sites was fed into Ensembl Variant Effect Predictor (VEP) [35] to identify associated amino acid changes, accounting for the strandness of the reads.

Statistical analyses

Normalization for heatmap and the statistical tests were executed in R (version 3.4.2). Differences between groups were assessed by a two-tailed Student’s *t*-test. A *p*-value ≤ 0.05 was considered statistically significant. Where indicated, the results are expressed as the mean \pm SD of three or more samples.

Synergism, additive effects, or antagonism were assessed by the Chou-Talalay method, utilizing CalcuSyn software (Biosoft). The average CI value for the experimental combination was calculated from the 50, 75, and 90% dose-effect levels of cell growth inhibition. By this method, CI values indicate the following: 0.3 - 0.7, strong synergism; 0.7–0.85, moderate synergism; 0.85–0.9, slight synergism; 0.9–1.1, nearly additive; 1.1–1.2, slight antagonism; 1.2–1.45, moderate antagonism; 1.45–3.3, antagonism; 3.3–10, strong antagonism [23].

Data availability

The CAGE and RNA-seq data generated during this study have been deposited to GEO under the access codes GSE149962 and GSE151249

Results

Primary AML cells bearing *FLT3*-ITD/D835 mutations show a higher frequency of co-mutations and higher levels of *BCL2A1* gene transcripts

To investigate differences in transcriptome and co-mutation profiles in primary AML patient cells bearing *FLT3*-ITD and *FLT3*-ITD/D835 mutations, we obtained cells from 26 patients (14 bearing *FLT3*-ITD and 12 bearing *FLT3*-ITD/D835 mutations). Table 1 summarizes clinical characteristics. Gene panel sequencing showed that co-mutations were identified more frequently in primary AML cells bearing *FLT3*-ITD/D835 mutations than cells bearing *FLT3*-ITD alone (Table 1). In particular, mutations in *RAS*, *ASXL1*, and *TET2* frequently co-existed in AML cells with *FLT3*-ITD/D835 mutations.

To investigate transcriptome profiles, CAGE transcriptome analyses were performed. CAGE peaks indicate transcription start sites, which allows the investigation of differentially expressed transcripts and

Table 1
Clinical characteristics and mutation status of primary AML samples.

Patient number	Diagnosis	Sex/Age (y)	Prior therapy	Mutation status <i>FLT3</i> -ITD /VAF (%)	<i>FLT3</i> -D835 /VAF (%)	Other genes*
1	AML	M/39	AML (3 + 7; DHAD+VP-16; DAC; AraC+TOPO)	Positive/47.0	Negative	Not detected
2	AML	F/86	None	Positive/47.5	Negative	Not detected
3	AML	M/32	AML (FLAG+Gemtuzumab ozogamicin)	Positive/24.3	Negative	Not detected
4	AMOL	M/81	None	Positive/24.9	Negative	Not detected
5	AMML	F/40	None	Positive/15.4	Negative	Not detected
6	AMML	F/55	None	Positive/47.9	Negative	Not detected
7	AMML	M/78	None	Positive/48.2	Negative	Not detected
8	AMML	F/62	None	Positive/48.2	Negative	Not detected
9	APL	F/36	None	Positive/ Positive**	Negative	Not detected
10	AML	M/46	None	Positive/2.1	Negative	<i>RAS</i>
11	AML	M/71	None	Positive/43.6	Negative	<i>CEBPA</i>
12	AML	M/47	None	Positive/1.6	Negative	<i>KIT</i>
13	AMOL	F/50	None	Positive/43.7	Negative	<i>RAS</i>
14	AMML	M/29	None	Positive/29.1	Negative	<i>RAS</i>
15	AML	M/32	AML (FLAG+Gemtuzumab ozogamicin)	Positive/24.3	Positive/ Positive**	Not detected
16	AMOL	F/51	AML (FLAG+IDA/AZA; FLAG+IDA/BMT; Sorafenib; Clofa+AraC)	Positive/46.0	Positive/33.8	Not detected
17	AML	F/87	AML (Hydrea+AraC; AraC+ DXR; Sorafenib)	Positive/39.6	Positive/13.3	<i>TET2, RUNX1, RAS</i>
18	AML	M/66	AML	Positive/6.4	Positive/3.4	<i>TET2, RUNX1, IKZF2, EZH2, RAS</i>
19	AML	M/81	None	Positive/3.1	Positive/34.9	<i>CEBPA, DNMT3, IDH2, MPL, RUNX1</i>
20	AML	M/76	ET (hydroxyurea)→AML (DAC+RUX)	Positive/46.3	Positive/3.9	<i>ASXL1, RUNX1, TET2, WT1</i>
21	AML	M/62	AML(3 + 7)	Positive/1.7	Positive/13.1	<i>IDH2, RAS</i>
22	AML	M/32	None	Positive/24.3	Positive/ Positive**	<i>CEBPA</i>
23	AML	M/24	AML (3 + 7; VP-16+Ctx; Quizartinib)	Positive/54.3	Positive/29.4	<i>IDH1, RAS</i>
24	AML	M/58	MDS (AZA), AML (3 + 7; Quizartinib)	Positive/87.3	Positive/50.1	<i>ASXL1, MLL, NOTCH1</i>
25	APL	M/80	Unknown	Positive/39.4	Positive/6.9	<i>DNMT3, EGFR, MPL</i>
26	APL	F/51	Unknown	Positive/2.0	Positive/27.7	<i>EGFR, EZH2, MLL, MPL, NOTCH1, RUNX1, TET2, WT1</i>

AML, acute myelogenous leukemia; APL, acute promyelocytic leukemia; AMOL, acute monocytic leukemia; AMML, acute myelomonocytic leukemia; MDS, myelodysplastic syndromes; VAF, variant allele frequency; ET, essential thrombocythemia; DHAD, mitoxantrone; VP-16, etoposide; DAC, decitabine; AraC, cytarabine; TOPO, topoisomerase; DXR, daunorubicin; RUX, ruxolitinib; Ctx, cyclophosphamide; AZA, azacitidine; FLAG, fludarabine, cytarabine and granulocyte colony stimulating factor; IDA, idarubicin; BMT, blood or marrow transplantation; Clofa, clofarabin.

* All samples were wt-NPM. The mutational status of 25 genes was analyzed.

** Data are not available.

promoter activities across the whole genome [32]. Out of 18,032 promoters, CAGE identified 310 upregulated and 22 downregulated promoters with a false discovery rate (FDR) of < 0.05 in AML cells bearing *FLT3*-ITD/D835 compared to cells bearing *FLT3*-ITD mutation. We then extracted 60 upregulated and 13 downregulated promoters that were functionally annotated by mammalian genomes, FANTOM 5 (Table 2) [36]. The expression levels of promoters for each sample are shown in a heatmap, and the differences between AML cases bearing *FLT3*-ITD and *FLT3*-ITD/D835 are demonstrated by a MA-plot diagram (Supplementary Figs. S1 and S2). The gene ontology (GO) analyses by Database for Annotation, Visualization, and Integrated Discovery (DAVID) [33] identified apoptotic pathways as the top GO term with 14 promoters (Fig. 1A and Supplementary Table S1). The promoter of *BCL2A1*, a *BCL-2* family gene, was one of the upregulated promoters in the AML cells bearing *FLT3*-ITD/D835 when compared to cells bearing *FLT3*-ITD alone (FDR < 0.05, log fold change > 2.0). Fig. 1B shows the profiles of promoter expressions of *BCL2A1* (left panel) and *BCL2* (right panel). In AML cells bearing *FLT3*-ITD/D835, *BCL2A1* transcripts were higher in cells with co-mutations than in cells without co-mutations. To examine the effects of upregulated *BCL2A1* promoters, mRNA levels were determined by qPCR. The left panel of Fig. 1C shows that the *BCL2A1* gene expression was upregulated in AML cells bearing *FLT3*-ITD/D835 compared to AML cells bearing *FLT3*-ITD mutation ($p = 0.03$). In contrast, the gene expression levels of *BCL2* were comparable between the AML cells bearing *FLT3*-ITD and bearing *FLT3*-ITD/D835 (right panel) ($p = 0.43$).

Upregulation of *BCL2A1* and increased confounding gene mutations in MV4;11 cells bearing *FLT3*-ITD/D835

We then examined the differences in mRNA and protein expression levels of *BCL2A1* and *BCL2* in isogenic MV4;11 cells bearing *FLT3*-ITD (MV4;11-ITD) and bearing *FLT3*-ITD/D835 mutations (MV4;11-ITD/D835). Fig. 2A shows that mRNA levels of *BCL2A1* were higher in MV4;11-ITD/D835 compared to MV4;11-ITD (left panel, $p < 0.01$) while mRNA levels of *BCL2* were comparable between the two groups (middle panel, $p = 0.05$). Concordant with these results, the western blot analyses showed that *BCL2A1* expression was 1.6-fold higher in MV4;11-ITD/D835 compared to MV4;11-ITD cells (Fig. 2A right panel), while *BCL2* protein expression was comparable between the two groups. In contrast, expressions of MCL-1 and BCL-XL levels were decreased in MV4;11-ITD/D835 compared to MV4;11-ITD. MV4;11-ITD/D835 cells have been established by the prolonged exposure to quizartinib, and our observation was consistent with our previous report that quizartinib downregulates the expression of MCL-1 and BCL-XL [37].

We further compared occurrence of co-mutations in the aforementioned cells. Compared to MV4;11-ITD, RNA-Seq analysis detected newly acquired mutations in MV4;11-ITD/D835 including *CCZ1* c.538C>A:(p.H180N), *PTPN11* c.218C>T:(p.T73I), *ZNF598* c.1675C>T:(p.P559S), *DDX5* c.427G>T:(p.G143W), and *ARFGAP3* c.1421G>A:(p.S474N).

Table 2CAGE-defined promoters differentially expressed between primary AML cells bearing *FLT3*-ITD and cells bearing *FLT3*-ITD/D835 (log2 FC > |2|, FDR < 0.05).

CAGE-defined promoter Upregulated (<i>FLT3</i> -ITD/D835 vs. <i>FLT3</i> -ITD)	Log2 FC	P value	FDR	CAGE-defined promoter Downregulated (<i>FLT3</i> -ITD/D835 vs. <i>FLT3</i> -ITD)	Log2 FC	P value	FDR
p1@TKTL1	8.22	3.61E-07	3.92E-03	p5@CD1E	-6.38	1.49E-05	2.10E-02
p5@H1F0	6.09	6.00E-05	4.29E-02	p1@CLIP3	-6.05	5.90E-05	4.26E-02
p3@SCGB3A1	5.76	6.58E-05	4.46E-02	p3@CYB5R3	-6.04	4.09E-05	3.47E-02
p1@C6orf126	5.39	9.38E-06	1.56E-02	p1@CD1B	-6.04	4.35E-05	3.58E-02
p6@QPCT	5.25	4.98E-06	1.17E-02	p2@KCNA5	-5.83	7.01E-05	4.58E-02
p5@LTF	5.11	7.50E-06	1.43E-02	p1@CD1E	-5.32	5.57E-05	4.20E-02
p2@S100A8	4.80	1.63E-07	3.66E-03	p1@PCDHGB5	-5.08	1.30E-05	1.92E-02
p1@D4S234E	4.60	5.19E-06	1.20E-02	p2@SLC4A3	-5.07	1.00E-05	1.63E-02
p4@NSMAF	4.30	2.98E-08	1.20E-03	p1@PPM1J	-4.89	6.48E-05	4.46E-02
p2@AATK	4.26	4.02E-05	3.44E-02	p1@TIMP4	-4.05	2.37E-06	8.02E-03
p13@NSMAF	3.95	6.93E-06	1.35E-02	p2@SIGLEC6	-3.93	6.24E-06	1.29E-02
p2@PNPLA2	3.94	4.19E-06	1.06E-02	p3@SOCS2	-3.89	8.16E-05	4.99E-02
p3@SRGN	3.93	1.73E-05	2.31E-02				
p9@TLR4	3.91	4.88E-05	3.81E-02				
p4@PRKCH	3.86	2.90E-07	3.92E-03				
p1@AK124679	3.84	6.47E-06	1.29E-02				
p1@HRH4	3.69	1.23E-05	1.90E-02				
p2@FCAR	3.66	9.27E-07	5.68E-03				
p3@EVI2B	3.64	2.74E-05	2.83E-02				
p4@CYP4F3	3.60	3.79E-05	3.36E-02				
p2@PRKCH	3.53	4.63E-05	3.69E-02				
p6@C2orf55	3.44	5.80E-05	4.24E-02				
p1@CD24	3.41	2.33E-05	2.67E-02				
p4@NFIL3	3.20	2.39E-07	3.92E-03				
p5@ANXA1	3.20	5.68E-06	1.25E-02				
p1@OLR1	3.13	6.21E-05	4.38E-02				
p1@OPLAH	3.13	6.54E-05	4.46E-02				
p3@RPL12	3.08	2.72E-06	8.45E-03				
p2@GPR160	2.99	6.50E-07	5.47E-03				
p4@CTSS	2.97	2.42E-05	2.71E-02				
p3@SYNE1	2.94	2.52E-06	8.08E-03				
p3@SLC36A4	2.90	3.02E-07	3.92E-03				
p3@ALOX5AP	2.87	4.22E-05	3.54E-02				
p2@NBN	2.85	8.40E-06	1.49E-02				
p7@KLF6	2.85	2.29E-05	2.67E-02				
p4@ALOX5	2.84	2.12E-05	2.60E-02				
p2@ENTPD1	2.82	1.29E-05	1.92E-02				
p1@LOC100130597	2.82	3.78E-05	3.36E-02				
p7@PLD1	2.75	6.65E-05	4.47E-02				
p3@GRK6	2.74	2.16E-05	2.63E-02				
p4@BCL2A1	2.74	4.54E-05	3.68E-02				
p17@TRIB1	2.74	5.33E-06	1.20E-02				
p1@DAPK2	2.74	3.80E-05	3.36E-02				
p1@CEACAM1	2.71	2.72E-05	2.83E-02				
p7@JMJD6	2.71	2.32E-05	2.67E-02				
p1@NAMPT	2.61	2.05E-05	2.56E-02				
p6@DYSF	2.60	2.18E-05	2.63E-02				
p2@RPS8	2.57	5.66E-05	4.20E-02				
p3@CHD7	2.56	2.44E-06	8.02E-03				
p5@RBM7	2.54	2.68E-05	2.83E-02				
p8@FGD4	2.50	7.23E-05	4.63E-02				
p6@ECE1	2.48	3.16E-05	3.05E-02				
p9@ANKRD28	2.47	2.66E-05	2.83E-02				
p1@PADI4	2.36	1.98E-05	2.51E-02				
p8@TMSB4X	2.34	6.65E-05	4.47E-02				
p4@CFL1	2.31	6.29E-05	4.40E-02				
p2@FLII	2.22	1.92E-05	2.46E-02				
p2@ACTG1	2.16	3.50E-05	3.23E-02				
p3@IFNGR1	2.08	2.80E-05	2.85E-02				
p2@CTBS	2.04	4.03E-05	3.44E-02				

FC, Fold Change; FDR, False Discovery Rate.

Upregulation of *BCL2A1* correlates with decreased sensitivity to quizartinib

To investigate whether drug resistance of AML cells bearing *FLT3*-ITD/D835 is associated with *BCL2A1*, we utilized Molm13 cells bearing the *FLT3*-ITD mutation and transfected with *BCL2A1* using lentiviral systems. Western blots confirmed that *BCL2A1* was overexpressed in the transfected cells, but not in the cells with mock transfections (Fig. 2B left panel). These cells were then treated with various concentrations of

quizartinib, and the apoptogenic effects were evaluated by Annexin V-FITC and compared to the cells with mock transfections. As shown in Fig. 2B (right panels), overexpression of *BCL2A1* significantly decreased the fraction of quizartinib-induced apoptotic Molm13 cells compared to the cells with mock transfection.

A phase Ib/II clinical trial using quizartinib, a Type II *FLT3* inhibitor, with venetoclax, a specific *BCL2* inhibitor, targeting AML with *FLT3*-ITD is ongoing (NCT03735875) and is showing encouraging results [18]. However, the effect of quizartinib combined with venetoclax specifically

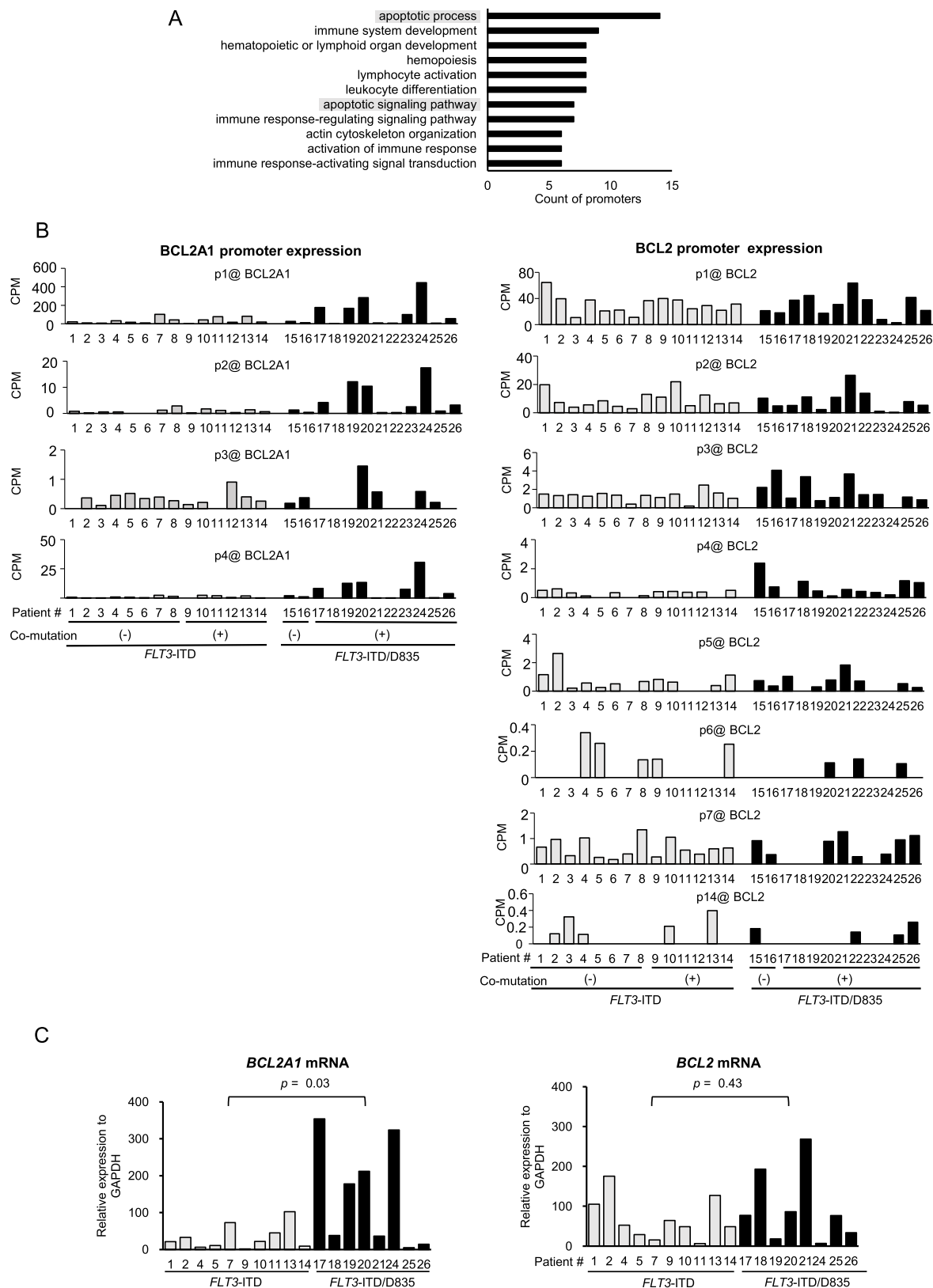


Fig. 1. Reference in promoter expression in primary AML cells bearing *FLT3*-ITD or *FLT3*-ITD/D835 mutations. (A) Gene ontology (GO) enrichment analysis of the biological process of up-regulated promoters using network DAVID. The top 10 GO terms relevant to biological process were sorted according to promoter counts and $p < 0.05$. (B) The y-axis shows counts per million (CPM) of human *BCL2A1* or *BCL2* promoters, detected by CAGE. The x-axis shows patient number. The patients in the *FLT3*-ITD or *FLT3*-ITD/D835 groups were further divided into groups with or without co-mutations. Peaks were given a name in the form pN@GENE, where GENE indicates gene name and N indicates alternative promoters of the same gene. (C) Transcript expression levels of either *BCL2A1* or *BCL2* in AML patients harboring the *FLT3*-ITD or *FLT3*-ITD/D835 mutations were confirmed by q-RT-PCR. The relative expression of each mRNA was normalized to GAPDH.

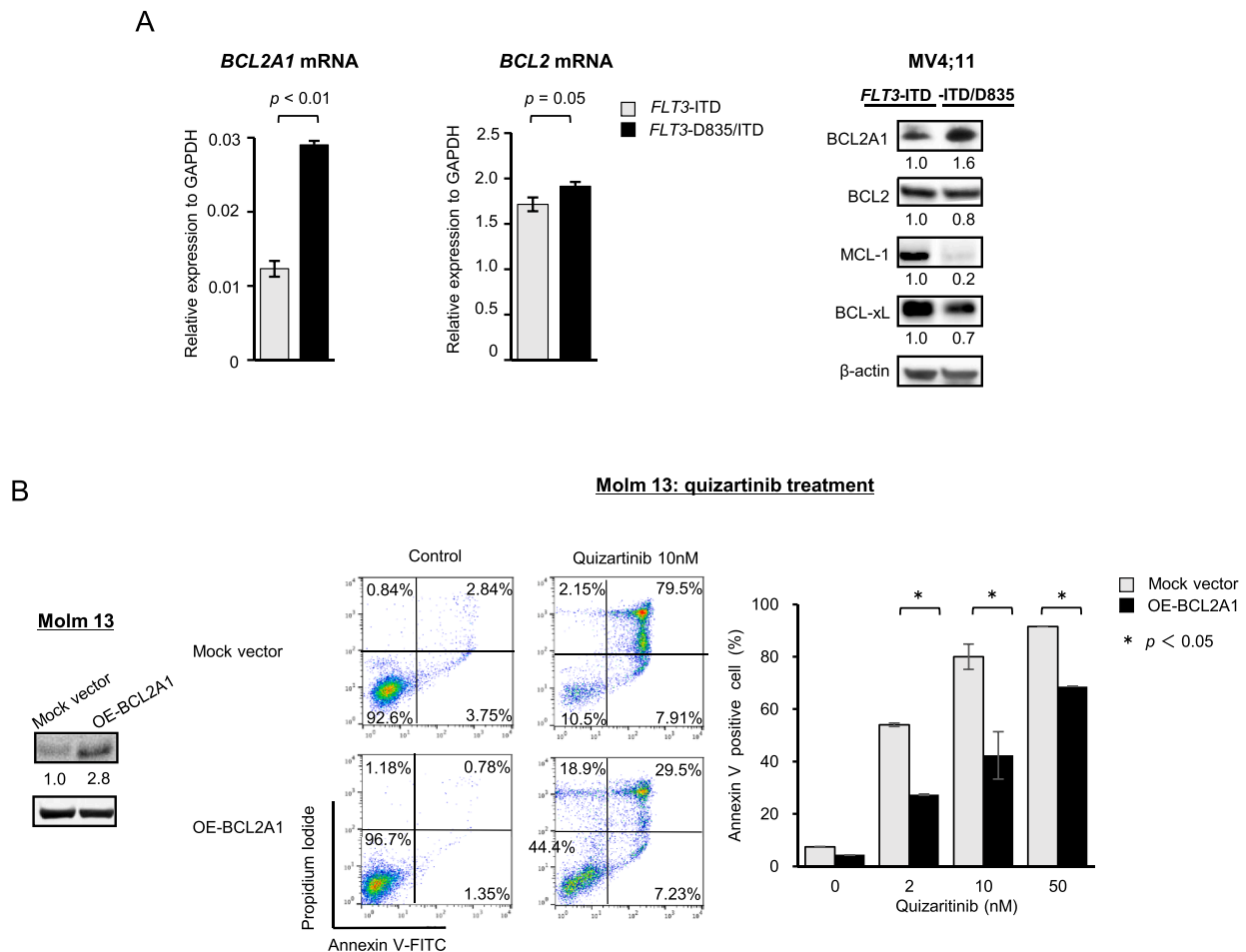


Fig. 2. (A) *BCL2A1* is upregulated in MV4;11-ITD/D835 compared to MV4;11-ITD/D835. *BCL2A1* and *BCL2* mRNA of MV4;11-ITD and MV4;11-ITD/D835 were detected by q-RT-PCR. The relative expressions of *BCL2A1* and *BCL2* mRNA were normalized by GAPDH. Protein expression levels of *BCL2A1*, *BCL2*, *MCL-1*, and *BCL-XL* in MV4;11-ITD and MV4;11-ITD/D835 were detected by immunoblotting. (B) Overexpression of *BCL2A1* attenuates quizartinib-induced cell growth inhibition and apoptosis in Molm13 cells. Comparative analysis of *BCL2A1* protein expressions in mock vector versus overexpressing (OE)-*BCL2A1* cell line was determined by western blot analysis. Molm13 cells with mock vector or OE-*BCL2A1* cells were treated with 2 to 50 nM quizartinib for 72 h. The percentages of annexin V-positive cells were evaluated by annexin V/PI (Propidium Iodide) staining and FACS analysis. Error bars, means \pm SD.

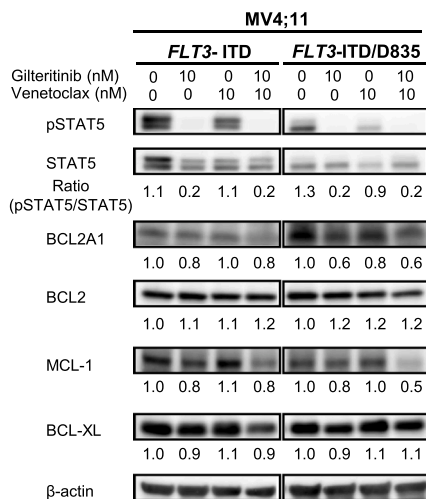
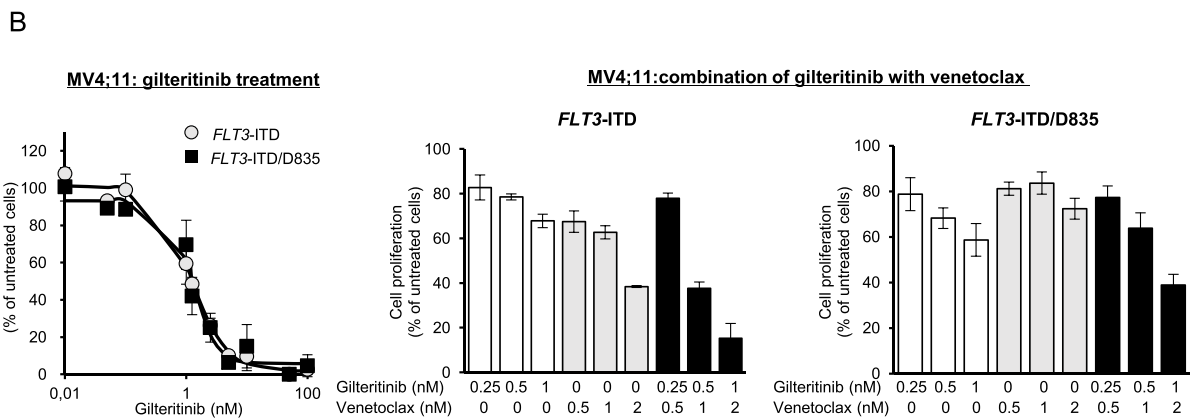
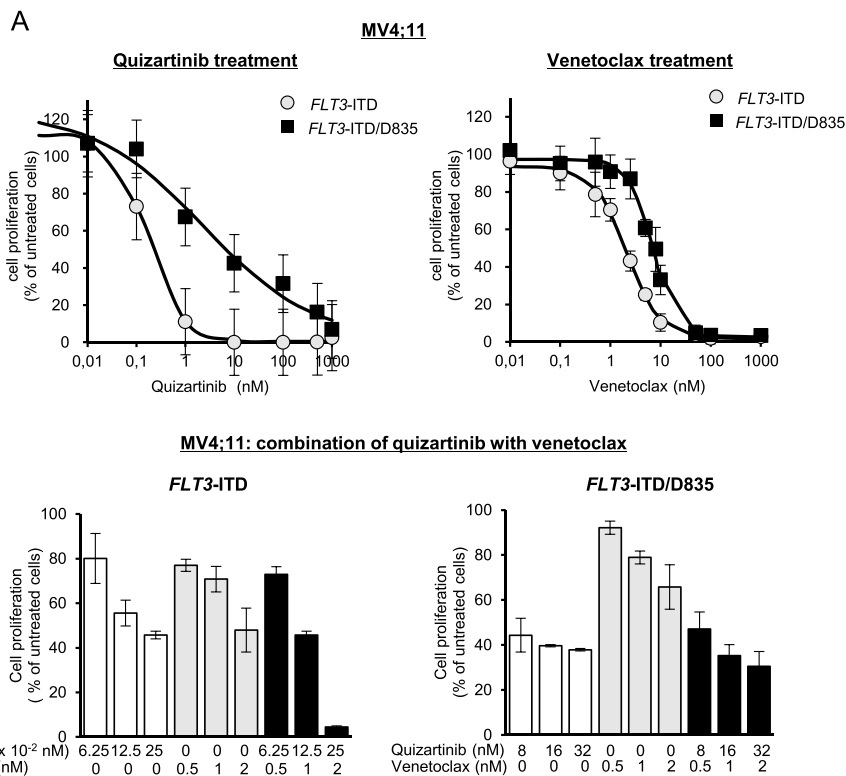
in AML with *FLT3*-ITD/D835 has not been well investigated. We therefore examined the dose-dependent inhibitory effects of quizartinib and venetoclax on cell proliferation of MV4;11-ITD or MV4;11-ITD/D835 (Fig. 3A). The top-left panel of Fig. 3A shows that MV4;11-ITD/D835 were significantly less sensitive to quizartinib compared to MV4;11-ITD (IC_{50} : 0.20 ± 0.02 nM vs. 7.69 ± 2.14 nM, $p < 0.01$, $n = 5$). The top-right panel of Fig. 3A shows that MV4;11-ITD/D835 were less sensitive than MV4;11-ITD to venetoclax (IC_{50} : 1.90 ± 0.58 nM vs. 6.78 ± 1.60 nM, $p < 0.01$, $n = 5$). This data is consistent with previous reports demonstrating that *BCL2A1* causes resistance to venetoclax [20,21]. We confirmed that overexpression of *BCL2A1* attenuated sensitivity of AML cells to venetoclax (Supplementary Fig. S3). The bottom panel of Fig. 3A shows effects of quizartinib in combination with venetoclax, on proliferation of MV4;11-ITD (left panel) and MV4;11-ITD/D835 cells (right panel). While proliferation of MV4;11-ITD was almost completely suppressed by the quizartinib (0.25 nM) and venetoclax (2 nM) combination in a synergistic manner (combination index, CI = 0.41), no synergistic combinational effects were observed in MV4;11-ITD/D835 (CI = 1.61).

Synergistic effects of gilteritinib and venetoclax on cell growth of MV4;11-ITD and MV4;11-ITD/D835

It has been shown that gilteritinib, a Type I *FLT3* inhibitor,

effectively blocks cell growth of AML cells bearing *FLT3*-ITD/D835 [38], and that the combination of gilteritinib and venetoclax is synergistically effective in AML cells with *FLT3*-ITD [39]. We therefore investigated the effects of gilteritinib and venetoclax on MV4;11-ITD and MV4;11-ITD/D835 cells.

The top-left panel of Fig. 3B shows that gilteritinib inhibited cell growth of MV4;11-ITD and MV4;11-ITD/D835 in a dose-dependent manner. The top-middle and right panels of Fig. 3B shows that combined treatment of gilteritinib and venetoclax synergistically reduced cell proliferation of both MV4;11-ITD and MV4;11-ITD/D835, although to a lesser degree in the double-mutant cells. To investigate underlying mechanism(s) of the combinational effects, we assessed protein levels of *STAT5*, a transcriptional regulator of *BCL2* family proteins [40,41]. As shown in Fig. 3B (bottom panel), western blot analysis demonstrated that treatment with gilteritinib only diminished phosphorylation of *STAT5* (p-*STAT5*) and decreased *BCL2A1* levels in both MV4;11-ITD and MV4;11-ITD/D835 cells. The combination of gilteritinib and venetoclax further downregulated *MCL-1* in MV4;11-ITD/D835. These results indicate that downregulation of p-*STAT5* and its downstream *BCL2* family proteins may be associated with the anti-leukemic effects of gilteritinib in AML cells bearing *FLT3*-ITD and *FLT3*-ITD/D835.



(caption on next page)

Fig. 3. (A) Cell growth inhibition by quizartinib and/or venetoclax in MV4;11-ITD and MV4;11-ITD/D835. MV4;11-ITD or MV4;11-ITD/D835 were treated with 0.01 to 1000 nM quizartinib or 0.01 to 1000 nM venetoclax and cell growth was assessed by the WST-8 test at 72 h. The concentration of drug resulting in 50% cell growth inhibition (IC_{50}) was calculated using CalcuSyn software (BioSoft, Cambridge, UK) from five independent experiments. IC_{50} of quizartinib: *FLT3*-ITD 0.20 ± 0.02 nM, *FLT3*-ITD/D835 7.69 ± 2.14 nM. IC_{50} of venetoclax: *FLT3*-ITD 1.90 ± 0.58 nM, *FLT3*-ITD/D835 6.78 ± 1.60 nM (top panels). *FLT3*-ITD positive cells or *FLT3*-ITD/D835-positive MV4;11 cells were treated for 72 h with 0.0625–32 nM quizartinib and/or 0.5–2 nM venetoclax, and cell growth was assessed by the WST-8 test. Combination index (CI) was calculated using CalcuSyn software. CI: *FLT3*-ITD 0.41, *FLT3*-ITD/D835 1.61 (bottom panels). (B) Synergistic cell growth inhibition by gilteritinib plus venetoclax. MV4;11-ITD or MV4;11-ITD/D835 were treated with 0.01 to 1000 nM gilteritinib and cell growth was assessed by the WST-8 test at 72 h. IC_{50} : *FLT3*-ITD 1.61 ± 0.63 nM, *FLT3*-ITD/D835 1.55 ± 0.98 nM (top-left panel). MV4;11-ITD or MV4;11-ITD/D835 were treated for 72 h with 0.25–1 nM gilteritinib and/or 0.5–2 nM venetoclax, and cell growth was assessed by the WST-8 test. CI: *FLT3*-ITD 0.23, *FLT3*-ITD/D835 0.28 (middle and right panels). Protein levels of p-STAT5 and anti-apoptotic family members were determined by western blot in MV4;11-ITD and MV4;11-ITD/D835 treated in the presence or absence of 10 nM gilteritinib and 10 nM venetoclax for 24 h. Error bars, means \pm SD.

Inhibition of bromodomain and extra-terminal motif (BET) induced apoptosis in MV4;11-ITD/D835

We next examined the anti-leukemic effects of CPI-0610, a BET inhibitor, known to exert anti-tumor effects by also inhibiting BCL2A1 [21]. Currently, no specific inhibitors of BCL2A1 are available, but a clinical trial using CPI-0610 for treatment of AML has been reported [42]. Fig. 4A shows that CPI-0610 inhibited cell growth dramatically with a modest increase in apoptosis in MV4;11-ITD (IC_{50} 256 \pm 87.4 nM) and MV4;11-ITD/D835 (IC_{50} 304 \pm 119 nM) in a dose dependent manner. Western blot analysis demonstrated that CPI-0610 decreased BCL2A1 in both cells (Fig. 4B).

Discussion

In this study, we asked the question: what factors are involved in the well-established resistance of double-mutated *FLT3*-ITD/D835 AML cells compared to that with *FLT3*-ITD only? We conducted a systemic global analysis of transcription start sites using CAGE analysis or primary clinical samples. Comprehensive bioinformatics analysis revealed apoptosis resistance as a top pathway. Next, we demonstrated upregulation of BCL2A1 both at the transcriptional and protein levels in AML cells bearing *FLT3*-ITD/D835 mutations compared to ones with *FLT3*-

ITD mutation only. The upregulation of BCL2A1 was found to account for resistance of AML cells bearing *FLT3*-ITD/D835 mutations to quizartinib as well as to venetoclax. BCL2A1 has been reported to play an important role in tumor expansion and/or metastasis of various solid cancers [43,44], hematopoietic malignancies [20,45], and resistance to venetoclax [20,21]. Indeed, the combination of quizartinib and venetoclax was not effective in AML cells bearing *FLT3*-ITD/D835 that highly express BCL2A1. However, the combination of gilteritinib and venetoclax showed synergistic effects in AML cells bearing *FLT3*-ITD/D835. We confirmed that gilteritinib reduced the expressions of p-STAT5 and BCL2A1 in MV4;11 cells bearing *FLT3*-ITD/D835. The expression of BCL2A1 is known to be regulated through JAK/STAT signaling [46,47] and here it is demonstrated that gilteritinib, at least in part, overcomes resistance of AML cells with *FLT3*-ITD/D835 to venetoclax by inhibition of JAK/STAT-BCL2A1 signaling.

While BCL2A1 may be a promising therapeutic target in AML with *FLT3*-ITD/TKD mutations, specific BCL2A1 inhibitors are currently unavailable. AML cells are vulnerable to BET family/BRD4 inhibitors, which transcriptionally suppress the expression of BCL2A1 and also downregulate the activity of important cell survival factors, such as MYC, BCL2, and CDK6 that are highly expressed in AML cells [21,48]. We observed that CPI-0610, a BET inhibitor [27], showed anti-tumor effects on AML cells bearing *FLT3*-ITD and *FLT3*-ITD/D835. Recently,

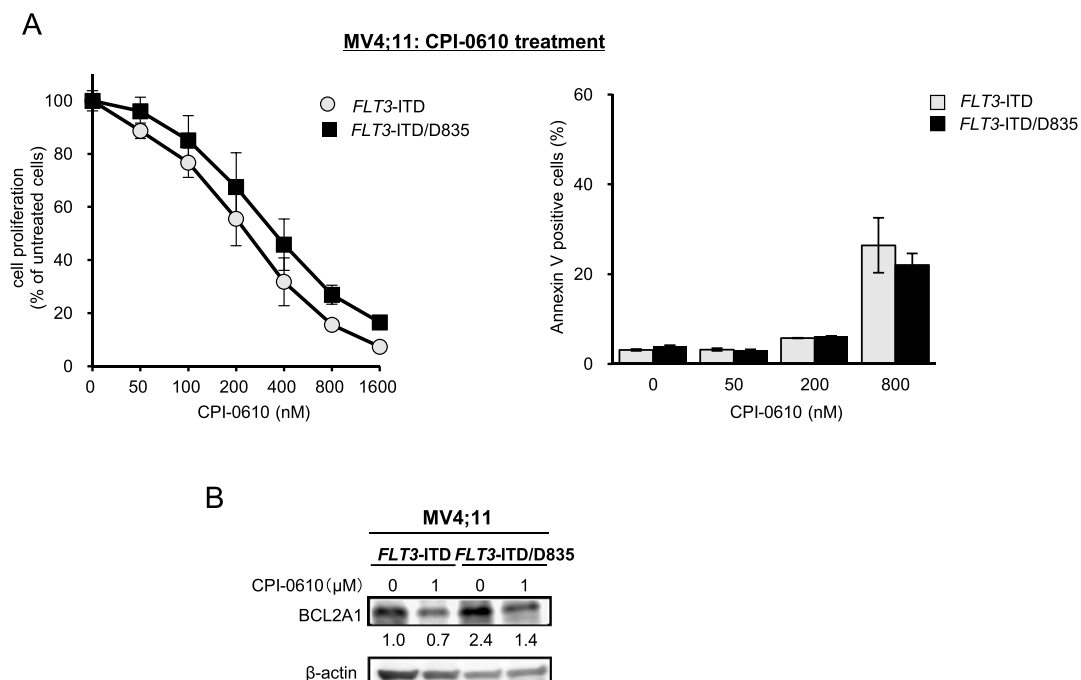


Fig. 4. BET inhibitor CPI-0610 effectively inhibits cell growth in MV4;11 cells regardless of the *FLT3*-ITD or *FLT3*-ITD/D835 mutation status. (A) MV4;11-ITD or MV4;11-ITD/D835 were treated with 50 to 1600 nM CPI-0610 for 72 h. Cell growth was assessed by the WST-8 test. The concentration of CPI-0610 resulting in 50% cell growth inhibition (IC_{50}) was calculated using CalcuSyn software. IC_{50} : *FLT3*-ITD 256 \pm 87.4 nM, *FLT3*-ITD/D835 304 \pm 119 nM. The percentages of apoptotic cells were analyzed by FACS analysis after stained with annexin V-FITC and propidium iodide (PI). Error bars, means \pm SD. (B) Protein levels of BCL2A1 were determined by western blot in MV4;11-ITD or MV4;11-ITD/D835 treated in the presence or absence of 1 μ M CPI-0610 for 24 h.

a combinatorial therapy of INCB054329, a novel BET inhibitor, and venetoclax has been shown to successfully reduce cell viability of AML cells associated with reduced transcriptional activation of key oncogenes as well as with genes involved in cell cycle and metabolism [49]. The promoter regions of *MYC* and *BCL2A1* contain BRD4 binding sites, suggesting that these genes are potentially sensitive to BRD4 inhibition [48]. BRD4 also activates NFκB via binding to the NFκB co-activator RELA [50], which is known to induce transcription of *BCL2A1* [51]. These studies and our findings reported here may explain the anti-tumor effects of BET inhibitors on AML cells with upregulated *BCL2A1*.

In our data, co-mutations in the genes, *RAS*, *ASXL1*, and *TET2*, were frequently detected in primary AML cells bearing *FLT3-ITD/D835* mutations. These findings are consistent with a previous study of the crenolanib-resistant cases exhibiting greater numbers of coexisting driver mutations in the *TET2*, *IDH1*, *RAS*, and *ASXL1* genes compared to the responders [52]. Similarly, *RAS* mutations were frequently found in the relapsed cases after treatment with gilteritinib [14]. Recently, Zhang *et al.* reported that *NRAS* mutations induced resistance against venetoclax by upregulating of *BCL2A1* through activation of NFκB signaling [53].

This study has significant limitations: (1) western blot analyses were only performed in cell lines because of inadequate amounts of primary patient samples in our repository; and (2) roles of other co-mutations detected in refractory AML samples could not be addressed though these mutations may be related to overexpression of *BCL2A1*. We are currently planning to address these issues in future projects.

In summary, we demonstrated that *BCL2A1* was upregulated in AML cells bearing *FLT3-ITD/TKD* mutations, which is a novel underlying mechanism of drug resistance. A combination of gilteritinib and venetoclax that suppresses *BCL2A1* has a potential to improve the prognosis of AML with *FLT3-ITD/D835* mutations. In addition, BET inhibitors that downregulate *BCL2A1* can be alternative reagents to treat AML bearing multiple mutations including *FLT3-ITD/D835*.

Financial support for this work

This work was supported in part by Grants-in Aid for Scientific Research (18J22436 to KY, 18K07424 to YT), International Joint Research Programs (19KK0221 to YT) from Japan Society for the Promotion of Science. This research was also partially supported by the Platform Project for Supporting Drug Discovery and Life Science Research (B Platform for Drug Discovery, Informatics, and Structural Life Science), and the Japan Agency for Medical Research and Development (AMED). Additional support was provided by the MD Anderson MDS/AML moonshot program, the CPRIT MIRA grant and funds from the Endowed Haas Chair in Genetics (all to MA).

CRedit authorship contribution statement

Kotoko Yamatani: Methodology, Investigation, Data curation, Formal analysis, Visualization, Funding acquisition, Writing – original draft. **Tomohiko Ai:** Methodology, Writing – review & editing. **Kaori Saito:** Investigation. **Koya Suzuki:** Methodology. **Atsushi Hori:** Methodology. **Sonoko Kinjo:** Formal analysis. **Kazuho Ikeo:** Formal analysis. **Vivian Ruvolo:** Methodology, Investigation, Resources. **Weiguo Zhang:** Methodology, Resources. **Po Yee Mak:** Methodology, Investigation, Resources. **Bogumil Kaczkowski:** Formal analysis. **Hironori Harada:** Methodology. **Kazuhiro Katayama:** Resources. **Yoshikazu Sugimoto:** Resources. **Jered Myslinski:** Formal analysis. **Takashi Hato:** Formal analysis. **Takashi Miida:** Methodology. **Marina Konopleva:** Methodology. **Yoshihide Hayashizaki:** Formal analysis, Methodology. **Bing Z. Carter:** Methodology, Investigation, Resources. **Yoko Tabé:** Conceptualization, Methodology, Formal analysis, Supervision, Writing – review & editing, Funding acquisition. **Michael Andreeff:** Conceptualization, Supervision, Funding acquisition.

Declaration of Competing Interest

MA has received research support from Daiichi-Sankyo; all other authors have no competing financial interests to declare.

Acknowledgments

The authors wish to thank the Laboratory of Molecular and Biochemical Research and Research Support Center at Juntendo University Graduate School of Medicine for technical assistance. We are also grateful to Dr. Toshiaki Takano and Dr. Hidetaka Eguchi from Intracetable Disease Research Center at Juntendo University Graduate School of Medicine for technical assistance. The authors would also like to thank Dr. Numsen Hail for assistance in editing the manuscript, Dr. Kaoru Mogushi, Dr. Masaki Hosoya, and Dr. Shigeo Yamaguchi for useful discussions.

Supplementary materials

Supplementary material associated with this article can be found, in the online version, at doi:10.1016/j.tranon.2022.101354.

References

- [1] A.A. Petti, S.R. Williams, C.A. Miller, I.T. Fiddes, S.N. Srivatsan, D.Y. Chen, et al., A general approach for detecting expressed mutations in AML cells using single cell RNA-sequencing, *Nat. Commun.* 10 (1) (2019) 3660, <https://doi.org/10.1038/s41467-019-11591-1>.
- [2] D.L. Stirewalt, J.P. Radich, The role of FLT3 in haematopoietic malignancies, *Nat. Rev. Cancer* 3 (9) (2003) 650–665, <https://doi.org/10.1038/nrc1169>.
- [3] U. Bacher, C. Haferlach, W. Kern, T. Haferlach, S. Schnittger, Prognostic relevance of FLT3-TKD mutations in AML: the combination matters—an analysis of 3082 patients, *Blood* 111 (5) (2008) 2527–2537, <https://doi.org/10.1182/blood-2007-05-091215>.
- [4] C. Thiede, C. Studel, B. Mohr, M. Schaich, U. Schakel, U. Platzbecker, et al., Analysis of FLT3-activating mutations in 979 myelogenous leukemia: association with FAB subtypes and identification of subgroups with poor prognosis, *Blood* 99 (12) (2002) 4326–4335, <https://doi.org/10.1182/blood.v99.12.4326>.
- [5] D. Staudt, H.C. Murray, T. McLachlan, F. Alvaro, A.K. Enjeti, N.M. Verrills, et al., Targeting oncogenic signaling in mutant FLT3 acute myeloid leukemia: the path to least resistance, *Int. J. Mol. Sci.* 19 (10) (2018), <https://doi.org/10.3390/ijms19103198>.
- [6] W. Zhang, M. Konopleva, Y.X. Shi, T. McQueen, D. Harris, X. Ling, et al., Mutant FLT3: a direct target of sorafenib in acute myelogenous leukemia, *J. Natl. Cancer Inst.* 100 (3) (2008) 184–198, <https://doi.org/10.1093/jnci/djm328>.
- [7] J.E. Cortes, S. Khaled, G. Martinelli, A.E. Perl, S. Ganguly, N. Russell, et al., Quizartinib versus salvage chemotherapy in relapsed or refractory FLT3-ITD acute myeloid leukaemia (QuANTUM-R): a multicentre, randomised, controlled, open-label, phase 3 trial, *Lancet Oncol.* 20 (7) (2019) 984–997, [https://doi.org/10.1016/s1470-2045\(19\)30150-0](https://doi.org/10.1016/s1470-2045(19)30150-0).
- [8] A.E. Perl, G. Martinelli, J.E. Cortes, A. Neubauer, E. Berman, S. Paolini, et al., Gilteritinib or chemotherapy for relapsed or refractory FLT3-mutated AML, *N. Engl. J. Med.* 381 (18) (2019) 1728–1740, <https://doi.org/10.1056/NEJMoa1902688>.
- [9] R.M. Stone, S.J. Mandrekar, B.L. Sanford, K. Laumann, S. Geyer, C.D. Bloomfield, et al., Midostaurin plus chemotherapy for acute myeloid leukemia with a FLT3 mutation, *N. Engl. J. Med.* 377 (5) (2017) 454–464, <https://doi.org/10.1056/NEJMoa1614359>.
- [10] M. Levis, Midostaurin approved for FLT3-mutated AML, *Blood* 129 (26) (2017) 3403–3406, <https://doi.org/10.1182/blood-2017-05-782292>.
- [11] E.D. Pulte, K.J. Norsworthy, Y. Wang, Q. Xu, H. Qosa, R. Gudi, et al., FDA approval summary: gilteritinib for relapsed or refractory acute myeloid leukemia with a FLT3 mutation, *Clin. Cancer Res.* 27 (13) (2021) 3515–3521, <https://doi.org/10.1158/1078-0432.Ccr-20-4271>.
- [12] Y. Alvarado, H.M. Kantarjian, R. Luthra, F. Ravandi, G. Borthakur, G. Garcia-Manero, et al., Treatment with FLT3 inhibitor in patients with FLT3-mutated acute myeloid leukemia is associated with development of secondary FLT3-tyrosine kinase domain mutations, *Cancer* 120 (14) (2014) 2142–2149, <https://doi.org/10.1002/ncr.28705>.
- [13] C.C. Smith, A. Paguirigan, G.R. Jeschke, K.C. Lin, E. Massi, T. Tarver, et al., Heterogeneous resistance to quizartinib in acute myeloid leukemia revealed by single-cell analysis, *Blood* 130 (1) (2017) 48–58, <https://doi.org/10.1182/blood-2016-04-711820>.
- [14] C.M. McMahon, T. Ferng, J. Canaani, E.S. Wang, J.J.D. Morrisette, D.J. Eastburn, et al., Clonal selection with RAS pathway activation mediates secondary clinical resistance to selective FLT3 inhibition in acute myeloid leukemia, *Cancer Discov.* 9 (8) (2019) 1050–1063, <https://doi.org/10.1158/2159-8290.Cd-18-1453>.

- [15] K. Bagrintseva, S. Geisenhof, R. Kern, S. Eichenlaub, C. Reindl, J.W. Ellwart, et al., FLT3-ITD-TKD dual mutants associated with AML confer resistance to FLT3 PTK inhibitors and cytotoxic agents by overexpression of Bcl-x(L), *Blood* 105 (9) (2005) 3679–3685, <https://doi.org/10.1182/blood-2004-06-2459>.
- [16] C.H. Man, T.K. Fung, C. Ho, H.H. Han, H.C. Chow, A.C. Ma, et al., Sorafenib treatment of FLT3-ITD(+) acute myeloid leukemia: favorable initial outcome and mechanisms of subsequent nonresponsiveness associated with the emergence of a D835 mutation, *Blood* 119 (22) (2012) 5133–5143, <https://doi.org/10.1182/blood-2011-06-363960>.
- [17] R.S. Mali, Q. Zhang, R. DeFilippis, A. Cavazos, V.M. Kuruvilla, J. Raman, et al., Venetoclax combines synergistically with FLT3 inhibition to effectively target leukemic cells in FLT3-ITD+ acute myeloid leukemia models, *Haematologica* (2020), <https://doi.org/10.3324/haematol.2019.244020>.
- [18] J.R. Sillar, A.K. Enjeti, Targeting apoptotic pathways in acute myeloid leukaemia, *Cancers* 11 (11) (2019), <https://doi.org/10.3390/cancers11111660>. Basel.
- [19] N. Dayer, J.K. Altman, J. Maly, M. Levis, E. Ritchie, M. Litzow, et al., Efficacy and safety of venetoclax in combination with gilteritinib for relapsed/refractory FLT3-mutated acute myeloid leukemia in the expansion cohort of a phase 1b study, *Blood* 136 (Supplement 1) (2020) 20–22, <https://doi.org/10.1182/blood-2020-139705>.
- [20] R. Bisailon, C. Moison, C. Thiollier, J. Krosli, M.E. Bordeleau, B. Lehnertz, et al., Genetic characterization of ABT-199 sensitivity in human AML, *Leukemia* 34 (1) (2020) 63–74, <https://doi.org/10.1038/s41375-019-0485-x>.
- [21] A. Esteve-Arenys, J.G. Valero, A. Chamorro-Jorganes, D. Gonzalez, V. Rodriguez, I. Dlouhy, et al., The BET bromodomain inhibitor CPI203 overcomes resistance to ABT-199 (venetoclax) by downregulation of BFL-1/A1 in *in vitro* and *in vivo* models of MYC+/BCL2+ double hit lymphoma, *Oncogene* 37 (14) (2018) 1830–1844, <https://doi.org/10.1038/s41388-017-0111-1>.
- [22] K. Katayama, K. Noguchi, Y. Sugimoto, Heat shock protein 90 inhibitors overcome the resistance to Fms-like tyrosine kinase 3 inhibitors in acute myeloid leukemia, *Oncotarget* 9 (76) (2018) 34240–34258, <https://doi.org/10.18632/oncotarget.26045>.
- [23] T.C. Chou, Drug combination studies and their synergy quantification using the Chou-Talalay method, *Cancer Res.* 70 (2) (2010) 440–446, <https://doi.org/10.1158/0008-5472.Can-09-1947>.
- [24] T. Takahashi, K. Usuki, K. Matsue, H. Ohno, T. Sakura, R. Imanaka, et al., Efficacy and safety of quizartinib in Japanese patients with FLT3-ITD positive relapsed or refractory acute myeloid leukemia in an open-label, phase 2 study, *Int. J. Hematol.* 110 (6) (2019) 665–674, <https://doi.org/10.1007/s12185-019-02727-6>.
- [25] Food and drug administration, Prescription Drug Labeling Resources, Food and drug administration, 2022. <https://www.accessdata.fda.gov/drugsatfda>. (Accessed 5 January 2022). https://www.accessdata.fda.gov/drugsatfda/_docs/label/2018/211349s000lbl.pdf.
- [26] Food and drug administration, Prescription Drug Labeling Resources, Food and Drug Administration, 2022. <https://www.accessdata.fda.gov/drugsatfda>. (Accessed 5 January 2022). https://www.accessdata.fda.gov/drugsatfda/_docs/label/2016/208573s000lbl.pdf.
- [27] B.K. Albrecht, V.S. Gehling, M.C. Hewitt, R.G. Vaswani, A. Cote, Y. Leblanc, et al., Identification of a benzoisoxazolozepine inhibitor (CPI-0610) of the bromodomain and extra-terminal (BET) family as a candidate for human clinical trials, *J. Med. Chem.* 59 (4) (2016) 1330–1339, <https://doi.org/10.1021/acs.jmedchem.5b01882>.
- [28] M. Milella, S.M. Kornblau, Z. Estrov, B.Z. Carter, H. Lapillonne, D. Harris, et al., Therapeutic targeting of the MEK/MAPK signal transduction module in acute myeloid leukemia, *J. Clin. Investig.* 108 (6) (2001) 851–859, <https://doi.org/10.1172/JCI12807>.
- [29] L. Zhang, R.R. Singh, K.P. Patel, F. Stingo, M. Routbort, M.J. You, et al., BRAF kinase domain mutations are present in a subset of chronic myelomonocytic leukemia with wild-type RAS, *Am. J. Hematol.* 89 (5) (2014) 499–504, <https://doi.org/10.1002/ajh.23652>.
- [30] M. Warren, R. Luthra, C.C. Yin, F. Ravandi, J.E. Cortes, H.M. Kantarjian, et al., Clinical impact of change of FLT3 mutation status in acute myeloid leukemia patients, *Mod. Pathol.* 25 (10) (2012) 1405–1412, <https://doi.org/10.1038/modpathol.2012.88>.
- [31] M. Murata, H. Nishiyori-Sueki, M. Kojima-Ishiyama, P. Carninci, Y. Hayashizaki, M. Itoh, Detecting expressed genes using CAGE, *Methods Mol. Biol.* (2014) 1164: 67–1164:85, https://doi.org/10.1007/978-1-4939-0805-9_7.
- [32] A.R. Forrest, H. Kawaji, M. Rehli, J.K. Baillie, M.J. de Hoon, V. Hablerle, et al., A promoter-level mammalian expression atlas, *Nature* 507 (7493) (2014) 462–470, <https://doi.org/10.1038/nature13182>.
- [33] W. Huang da, B.T. Sherman, R.A. Lempicki, Systematic and integrative analysis of large gene lists using DAVID bioinformatics resources, *Nat. Protoc.* 4 (1) (2009) 44–57, <https://doi.org/10.1038/nprot.2008.211>.
- [34] E. Picardi, G. Pesole, REDtools: high-throughput RNA editing detection made easy, *Bioinformatics* 29 (14) (2013) 1813–1814, <https://doi.org/10.1093/bioinformatics/btt287>.
- [35] W. McLaren, L. Gil, S.E. Hunt, H.S. Riat, G.R. Ritchie, A. Thormann, et al., The ensemble variant effect predictor, *Genome Biol.* 17 (1) (2016) 122, <https://doi.org/10.1186/s13059-016-0974-4>.
- [36] S. Noguchi, T. Arakawa, S. Fukuda, M. Furuno, A. Hasegawa, F. Hori, et al., FANTOM5 CAGE profiles of human and mouse samples, *Sci. Data* 4 (2017), 170112, <https://doi.org/10.1038/sdata.2017.112>.
- [37] R. Singh Mali, Q. Zhang, R.A. DeFilippis, A. Cavazos, V.M. Kuruvilla, J. Raman, et al., Venetoclax combines synergistically with FLT3 inhibition to effectively target leukemic cells in FLT3-ITD+ acute myeloid leukemia models, *Haematologica* 106 (4) (2021) 1034–1046, <https://doi.org/10.3324/haematol.2019.244020>.
- [38] M. Mori, N. Kaneko, Y. Ueno, M. Yamada, R. Tanaka, R. Saito, et al., Gilteritinib, a FLT3/AXL inhibitor, shows antileukemic activity in mouse models of FLT3 mutated acute myeloid leukemia, *Investig. New Drugs* 35 (5) (2017) 556–565, <https://doi.org/10.1007/s10637-017-0470-z>.
- [39] J. Ma, S. Zhao, X. Qiao, T. Knight, H. Edwards, L. Polin, et al., Inhibition of Bcl-2 synergistically enhances the antileukemic activity of midostaurin and gilteritinib in preclinical models of FLT3-mutated acute myeloid leukemia, *Clin. Cancer Res.* 25 (22) (2019) 6815–6826, <https://doi.org/10.1158/1078-0432.Ccr-19-0832>.
- [40] J.V. Alvarez, D.A. Frank, Genome-wide analysis of STAT target genes: elucidating the mechanism of STAT-mediated oncogenesis, *Cancer Biol. Ther.* 3 (11) (2004) 1045–1050, <https://doi.org/10.4161/cbt.3.11.1172>.
- [41] G. Yoshimoto, T. Miyamoto, S. Jabbarzadeh-Tabrizi, T. Iino, J.L. Rocnik, Y. Kikushige, et al., FLT3-ITD up-regulates MCL-1 to promote survival of stem cells in acute myeloid leukemia via FLT3-ITD-specific STAT5 activation, *Blood* 114 (24) (2009) 5034–5043, <https://doi.org/10.1182/blood-2008-12-196055>.
- [42] A.G. Cochran, A.R. Conery, R.J. Sims, Bromodomains: a new target class for drug development, *Nat. Rev. Drug Discov.* 18 (8) (2019) 609–628, <https://doi.org/10.1038/s41573-019-0030-7>.
- [43] H.S. Yoon, S.H. Hong, H.J. Kang, B.K. Ko, S.H. Ahn, J.R. Huh, Bfl-1 gene expression in breast cancer: its relationship with other prognostic factors, *J. Korean Med. Sci.* 18 (2) (2003) 225–230, <https://doi.org/10.3346/jkms.2003.18.2.225>.
- [44] A.I. Riker, S.A. Enkemann, O. Fodstad, S. Liu, S. Ren, C. Morris, et al., The gene expression profiles of primary and metastatic melanoma yields a transition point of tumor progression and metastasis, *BMC Med. Genom.* 1 (2008) 13, <https://doi.org/10.1186/1755-8794-1-13>.
- [45] A.A. Morales, A. Olsson, F. Celsing, A. Osterborg, M. Jondal, L.M. Osorio, High expression of bfl-1 contributes to the apoptosis resistant phenotype in B-cell chronic lymphocytic leukemia, *Int. J. Cancer* 113 (5) (2005) 730–737, <https://doi.org/10.1002/ijc.20614>.
- [46] O. Cochet, C. Prelin, J.F. Peyron, V. Imbert, Constitutive activation of STAT proteins in the HDLM-2 and L540 Hodgkin lymphoma-derived cell lines supports cell survival, *Cell. Signal.* 18 (4) (2006) 449–455, <https://doi.org/10.1016/j.cellsig.2005.05.010>.
- [47] J. Vier, M. Groth, M. Sochalska, S. Kirschner, The anti-apoptotic Bcl-2 family protein A1/Bfl-1 regulates neutrophil survival and homeostasis and is controlled via PI3K and JAK/STAT signaling, *Cell Death Dis.* 7 (2) (2016) e2103, <https://doi.org/10.1038/cddis.2016.23>.
- [48] G. Jiang, W. Deng, Y. Liu, C. Wang, General mechanism of JQ1 in inhibiting various types of cancer, *Mol. Med. Rep.* 21 (3) (2020) 1021–1034, <https://doi.org/10.3892/mmr.2020.10927>.
- [49] H.E. Ramsey, D. Greenwood, S. Zhang, M. Childress, M.P. Arrate, A.E. Gorska, et al., BET inhibition enhances the antileukemic activity of low-dose venetoclax in acute myeloid Leukemia, *Clin. Cancer Res.* 27 (2) (2021) 598–607, <https://doi.org/10.1158/1078-0432.Ccr-20-1346>.
- [50] A. Hajmirza, A. Emadali, A. Gauthier, O. Casanovas, R. Gressin, M.B. Callanan, BET family protein BRD4: an emerging actor in NFκB signaling in inflammation and cancer, *Biomedicines* 6 (1) (2018), <https://doi.org/10.3390/biomedicines6010016>.
- [51] M. Vogler, BCL2A1: the underdog in the BCL2 family, *Cell Death Differ.* 19 (1) (2012) 67–74, <https://doi.org/10.1038/cdd.2011.158>.
- [52] H. Zhang, S. Savage, S.K. Schultz ARM, C.A. Eide, T. Nechiporuk, A. Carlos, et al., Clinical resistance to crenolanib in acute myeloid leukemia due to diverse molecular mechanisms, *Nat. Commun.* 10 (1) (2019) 244, <https://doi.org/10.1038/s41467-018-08263-x>.
- [53] H. Zhang, Y. Nakauchi, T. Köhnke, M. Stafford, D. Bottomly, R. Thomas, et al., Integrated analysis of patient samples identifies biomarkers for venetoclax efficacy and combination strategies in acute myeloid leukemia, *Nat. Cancer* 1 (8) (2020) 826–839, <https://doi.org/10.1038/s43018-020-0103-x>.